Global bifurcation destroying the experimental torus T^2

T. Pereira,[1,2] M. S. Baptista,[2] M. B. Reyes,[1] I. L. Caldas,[1] J. C. Sartorelli,[1] and J. Kurths[2]
[1]*Instituto de Física, Universidade de São Paulo Caixa Postal 66318, 05315-970 São Paulo, SP, Brazil*
[2]*Nonlinear Dynamics, Institute of Physics, University of Potsdam, D-14415, Potsdam, Germany*
(Received 28 April 2005; revised manuscript received 6 September 2005; published 11 January 2006)

We show experimentally the scenario of a two-frequency torus T^2 breakdown, in which a global bifurcation occurs due to the collision of a torus with an unstable periodic orbit, creating a heteroclinic saddle connection, followed by an intermittent behavior.

DOI: 10.1103/PhysRevE.73.017201 PACS number(s): 05.45.Tp, 05.45.Ac, 07.05.Kf

Chaotic behavior has been extensively studied in several areas of physical sciences [1], in economy [2], in ecology [3], and in applied engineering [4]. One important question toward the understanding of chaotic motion is the transition from a regular behavior to a chaotic one. This transition has been studied in conservative [5] and dissipative systems [1,6].

Among the ways chaotic behavior appears are the routes via the bifurcations of a quasiperiodic attractor with N incommensurate frequencies, also known as torus T^N. This route for the higher dimension torus, in which $N \geqslant 3$, has been well analyzed in Refs. [7,8]. For the low dimension torus T^2, chaos might appear by the Curry-Yorke scenario [9–11], and by torus doubling bifurcations [12]. A torus T^2 transition to chaos was also observed in a CO_2 laser [13].

Recently, Baptista and Caldas [14,15] have shown the appearance of chaotic behavior by an abrupt transition directly from the torus T^2, in which there is a collision of the torus with saddle points [16] originating an intermittent behavior. They argued that there is a mechanism of reinjection associated to a heteroclinic connection between the central unstable focus and the saddles, which takes the trajectory back to the vicinity of the focus. As reported by Letellier *et al.* [17], this phenomenon is not only restricted to continuous-time systems but it also happens in spatio-temporal systems.

In this work, we report experimental details of this scenario of T^2 breakdown. We show the global dynamics by identifying the collision of the torus with the saddle points, and by characterizing the local dynamics showing the existence of the focus and saddle points, i.e., the stretching and the folding character of the saddle vicinity, and the spiraling character of the focus vicinity. Finally, we also experimentally characterize the observed intermittency.

The forced Chua's circuit is composed of two capacitors, C_1 and C_2, two resistors, R and r, one inductor, L, and the nonlinear active (piecewise-linear) resistor, R_{NL} [14], whose characteristic curve is mathematically represented by $i_{NL}(V_{c1}) = m_0 V_{c1} + 0.5(m_1 - m_0)\{|V_{c1} + B_p| - |V_{c1} - B_p|\}$, where V_{c1} is the voltage in the capacitor C_1. The forcing applied to the circuit is of the form $V_p \sin(2\pi f_p t)$, where V_p is the amplitude and f_p is the frequency. More details about this circuit can be found in Ref. [18].

The circuit is constructed such that the characteristi curve presents $m_0 = -0.539(3)$ mA/V, $m_1 = -0.910(2)$ mA/V, and $B_p = 1.200(4)$ V. The number between brackets indicates the deviation in the last digit. The components of the circuit are $C_1 = 0.0047$ μF, $C_2 = 0.052$ μF, $R \in [1.0, 1.7] K\Omega$, $L = 9.2$ mH, and $r = 10$ Ω. We set the resistor R to obtain the regime of a double-Scroll-like attractor, and then we introduce the perturbation destroying this attractor, which gives place to the attractors observed in this work. We use a Tektronix AFG320 function generator connected in parallel to the resistor r, to introduce the forcing in the circuit. Data acquisition is performed using an AT-MIO 16E1 National Instruments board (12 bits) with a sampling of $\delta = 1/250$ kHz.

We acquire the variable $V_{c_1}(t = i\delta)$, with i representing the number of acquired data points. Next, we identify all its local maxima $V_{c_1}(n)$, where the n index represents the number of maxima. This time series $V_{c1}(n)$ is used to reconstruct the attractor $V_{c_1}(n) \times V_{c_1}(n+p)$, using time-delay embedding coordinates, with p representing the time delay for the embedding space. The value of p is chosen conveniently according to the geometry of the attractor studied, here $p = 2$. By working with this embedding, we can better visualize the attractors and the manifolds since this space has one dimension less than the usual phase space.

We use as control parameters the voltage V_p and frequency f_p of the forcing. As we change these parameters several windows of periodic motion appear. In particular, we explore the system close to the periodic window at $V_p = 0.7$ V and $f_p = 3500$ Hz. For $V_p = 0.7$ V fixed, we change f_p within the $[3505, 3537]$ Hz and build the bifurcation diagram as shown in Fig. 1. The periodic window remains up to $f_p = 3514$ Hz, when a Hopf bifurcation occurs. Further increasing the control parameter, at $f_p = 3530.6$ Hz (indicated by letter C) a sudden change in the system dynamics happens, the destruction of the torus by a torus-saddle collision, generating an intermittent behavior. Close to the Hopf bifurcation point, the torus has a circular shape. As the parameter is increased the torus shape becomes like a pentagon. This change happens when the torus grows and gets close to the five fixed points corresponding to a period-5 saddle orbit.

The existence of the saddle points, near this distorted torus, can be verified by introducing a small perturbation in the forced Chua's circuit, e.g., changing the magnetic flow in the inductor. This perturbation sets the trajectory apart from the attractor [19].

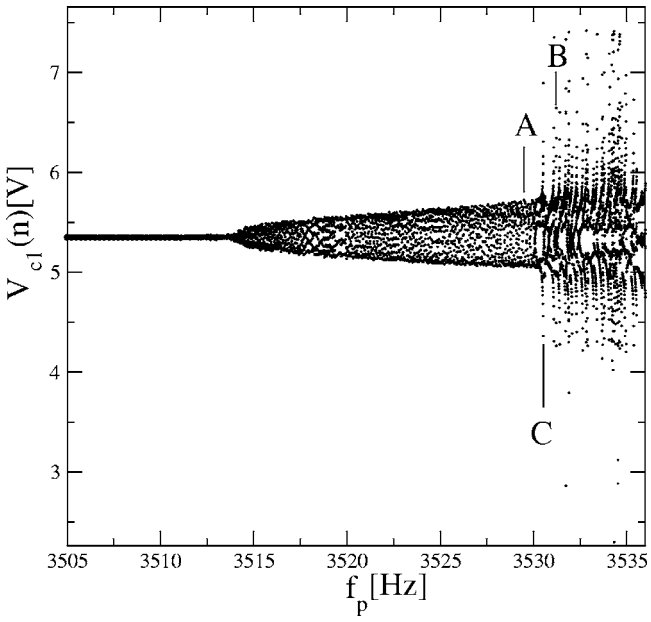

FIG. 1. Bifurcation diagram of the forced Chua's circuit, for V_p=0.7 V. One sees a fixed point that bifurcates by a Hopf bifurcation into a torus T^2. At a critical parameter f_p=3530.6 Hz, indicated by the letter C, a torus-saddle collision. The attractors indicated by the letters A and B are shown in Figs. 2 and 3, respectively.

With this procedure we are able to place the trajectory in the vicinity of the saddle points, as well as, in different parts of the phase space. We repeat this perturbation until we have a picture of the phase space in which we can clearly see the saddle points. Those are identified by selecting trajectory points that after p-iterations are mapped close by. In Fig. 2,

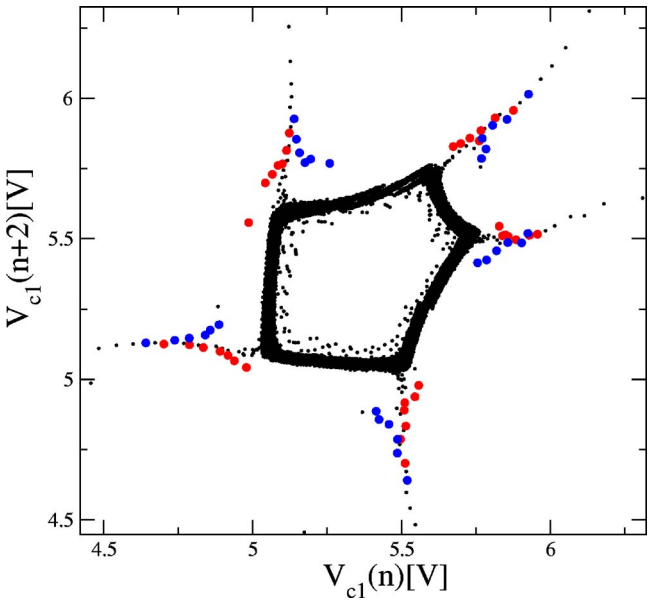

FIG. 2. (Color online) The pentagon-shape structure is the torus T_2, and with the small filled circles we show orbits that are placed in the vicinity of the saddle as we perturb the circuit. This takes the trajectories away from the torus and reveals the structure of the phase space near the torus, i.e., the existence of the saddles.

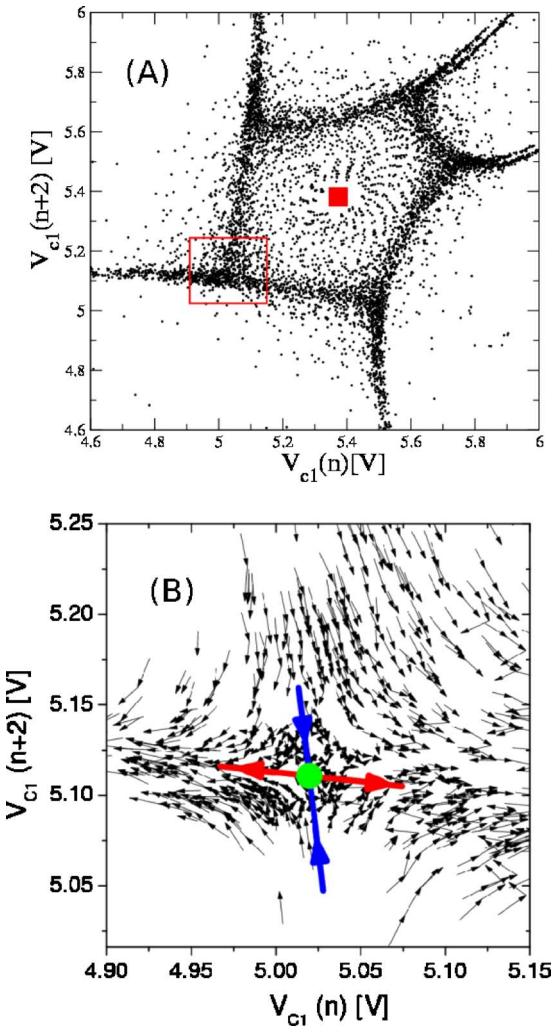

FIG. 3. (Color online) (A) The chaotic attractor born from a global bifurcation, the torus-saddle collision, for f_p=3531 Hz. The square in the center of the broken torus represents the unstable focus point. (B) We analyze the dynamics inside the small square in (A). The arrows connect a given point with its fifth iterate. One can see the saddle structure represented by the arrows, the unstable (stable) manifold is revealed by looking at the direction of the vectors. The filled circle indicates the saddle point position and the oversized arrows indicate the unstable and stable manifolds of the saddle point.

we show the torus that resembles a pentagon and the perturbed trajectories that are placed in the vicinity of the saddles. After reaching the saddle vicinities, the trajectory goes either toward the torus or away from it, by the stable or the unstable manifolds of the saddle points (filled circles), respectively. At a critical parameter f_p=3530.6 Hz, the torus collides with the external saddle points, it breaks and an intermittent behavior takes place. Analyzing the destroyed torus, depicted in Fig. 3(a), we can still detect the presence of the saddle points, which indicates that at the collision of the saddle with the torus T^2 a heteroclinic saddle connection is formed. That is done by analyzing the local geometry of the mapping around the saddle points, i.e., observing the return of a set of initial conditions around these saddles, after five iterations. In Fig. 3(b), inside the square shown in Fig. 3(a)

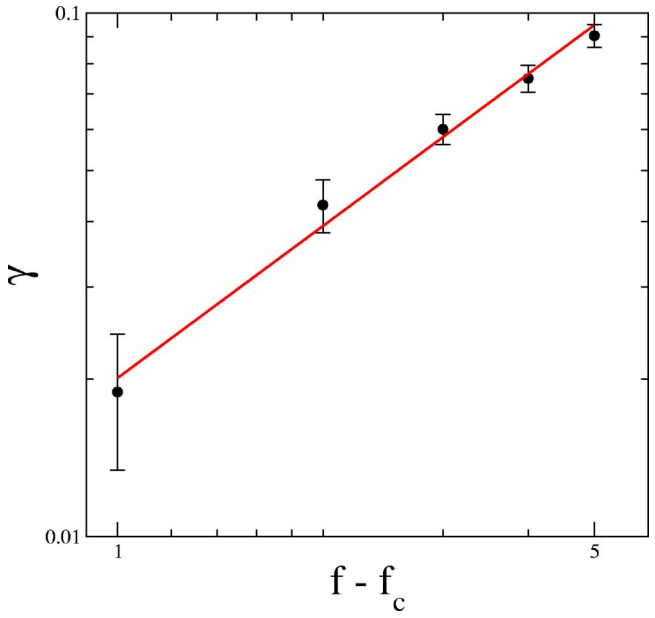

FIG. 4. (Color online) We show $\gamma \times |f-f_c|$, in a log × log graph. By fitting the data set, we have that the average laminar time scales as $\tau \propto |f-f_c|^{\mu}$, where $\mu=0.96$.

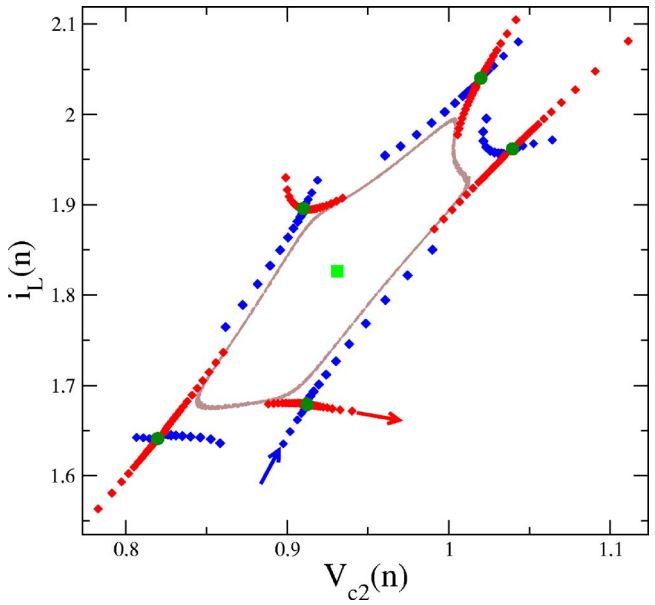

FIG. 5. (Color online) We show the torus (gray dots), the unstable focus (light gray square), the saddle points (filled circles), and a picture of the manifolds (diamonds) of the saddle points. These manifolds are depicted by iterating a set of initial conditions very close to one saddle point. The stable manifold of the saddles are indicated by dark diamonds (see the dark arrow), and the unstable manifolds are indicated by the gray diamonds (see the gray arrow).

we connect with arrows the points in the set of initial conditions and the corresponding returning points. We selected the shortest arrows in order not to overwhelm the picture, revealing the saddle.

We also see that the dynamics is still related to the torus. In fact, the trajectories behave as if they were in a quasiperiodic oscillation, near the saddle points, for a while. Then, they go away from the saddle vicinity along the saddle unstable manifolds, spending some time far away from the region delimited by the saddles. Finally, they are eventually reinjected in the unstable focus vicinity, spiraling toward the saddle points.

The unstable focus, in the attractor shown in Fig. 3(a), was obtained by the fixed point transform [20], which consists in transforming the original data set, such that the transformed data is concentrated on the periodic orbits. The histograms of the transformed data presents sharp peaks at the location of the unstable periodic orbits, which allow us to estimate their positions. The trajectories in the branches of the broken torus, the extended structures in Fig. 3(a), are governed by the unstable manifold of the saddle points. To see this, we evolve in time a set of points in the branch, close to the saddle, and after $k \times 5$ iterations, with k small, this set returns to the branch, but stretched. Following the consecutive iterates of the branches, we notice that the points on the branches are eventually mapped in the vicinity of the focus. The scaping of the trajectory from the saddles (chaotic bursts) and the subsequent reinjections around the focus generate the intermittent behavior.

In experimental situations, measuring the average laminar time, namely τ, can be rather problematic, as noted in Ref. [21], since one might mislead the determination of the laminar period, by working with variables that are in a projection of the full space. It is better to compute a more robust quantity called γ. This quantity measures the fraction of the time of the chaotic burst $\gamma=t_{\text{burst}}/t_{\text{total}}$ and, as the chaotic burst is very pronounced, the error in the statistics is smaller. Assuming $\tau \propto \epsilon^{-\mu}$, the variable γ is related to τ by $\gamma=[1+(d/\epsilon^{\mu})]^{-1}$ with d being a constant (see Ref. [21] for more details). Since $1 \ll d/\epsilon^{\mu}$, we can write $\gamma \propto \epsilon^{\mu}$. From our experimental results we have that $\mu=0.96$ (Fig. 4). Next, we estimate the Lyapunov exponents of our data through the Eckmann-Ruelle technique [6], by using the two-dimensional embedding $\{V_{c1}^{-}(n), V_{c1}(n+2)\}$. The spectra of the Lyapunov exponents, for the forced Chua's circuit has the form $\Lambda=(\lambda_1, 0, \lambda_2, -c)$. The null exponent corresponds to the direction of the flow, and the $-c$ exponent corresponds to the strong stable foliation. The other two exponents, λ_1 and λ_2, correspond to the stretching and the folding dynamics of the return map $V_{c1}(n) \times V_{c1}(n+2)$. The spectrum that corresponds to the attractor of Fig. 3 is $\lambda_1=0.30\pm0.08$ and $\lambda_2=-0.10\pm0.04$, with one positive Lyapunov exponent, and therefore chaotic behavior.

In order to have a better picture of the way the saddle points collide with the torus we perform numerical analysis of the circuit equations, with parameters that adequately reproduce the experimental scenario. The circuit equations can be obtained by applying the Kirchoff's laws. The resulting state equations are given by

$$C_1 \frac{dV_{c1}}{dt} = \frac{1}{R}(V_{c2} - V_{c1}) - i_{NR}(V_{C1}),$$

$$C_2 \frac{dV_{c2}}{dt} = \frac{1}{R}(V_{c1} - V_{c2}) + i_L,$$

$$L\frac{di_L}{dt} = -V_{c2} - V_p \sin\phi,$$

and

$$\frac{d\phi}{dt} = 2\pi f_p,$$

where V_{c1} and V_{c2} are the voltage in the capacitors C_1 and C_2, respectively, and i_L is the electric current across the inductor L.

The parameters used in the numerical simulation are $C_1 = 0.1$, $C_2 = 1.0$, $L = 1/6$, $1/R = 0.575$, $m_0 = -0.5$, $m_1 = -0.8$, and $B_p = 1.0$. The experimental scenario can be reproduced if we set the perturbation amplitude at $V = 0.234$ and change the frequency in the interval $f_p = [0.1775, 0.1795]$. The numerical analysis are done in a Poincaré section at $V_{c_1} = -1.5$. Plotting $V_{c_2}(n) \times f_p$ we obtain similar pictures as in the experimental scenario.

In order to detect the saddle points as well as the focus, we introduce a numerical technique, which can be adapted to experimental data series. The method consists in integrating the equations for several trials and changing the initial condition in each trial. The initial conditions are randomly chosen within a volume centered at a point p_0 in the chosen Poincaré section of the phase space. The point p_0 must be close to the searched period-n unstable orbit, the distance was set to be smaller than 10^{-8}. Applying this method we were able to detect the unstable periodic orbits of the flow, which gives place to the saddle points in the Poincaré section. The unstable orbit exists for all parameters within $f_p = [0.1775, 0.1795]$ and $V = 0.234$.

At a particular parameter $f_p = 0.178\,93$, we manage to get a local illustration of the manifolds of the saddle points. For that, we evolve forward and backward a small set of initial condition very close to a saddle point, just a few returns to the section. Then, having a better picture of the local structure of the manifolds, we choose new initial conditions, which are close to the manifolds and iterate them. The result is shown in Fig. 5, with the saddles indicated by the filled circles, coexisting with the pentagon-shape torus T^2 in gray dots. In this figure one can clearly see the distortion of the torus T^2 due the manifolds of the saddle points.

Concluding, we analyze experimentally the scenario of a two-frequency torus breakdown by a global bifurcation. We show (i) the existence of the saddle points; (ii) the existence of the focus point; (iii) a local picture of the manifolds of the saddle points; (iv) the verification of a power scaling law for the average laminar length, $\tau \propto |f - f_c|^{-0.96}$.

The authors thank M. J. Sotomayor and A. J. P. Fink for useful discussions. We acknowledge support from the the Alexander Humboldt Foundation (MSB), "Helmholtz Center for Mind and Brain Dynamics" (T.P. and J.K.), and FAPESP.

[1] E. Ott, *Chaos in Dynamical Systems* (Cambridge University Press, Cambridge, 1993); K. T. Alligood, T. D. Sauer, and J. A. Yorke, *Chaos, an Introduction to Dynamical Systems* (Springer, New York, 1997).
[2] P. De Grauwe, H. Wachter, and M. Embrechts, *Exchange Rate Theory: Chaotic Models of Foreign Exchange Markets* (Blackwell, Oxford, 1993).
[3] B. Blasius and L. Stone, Nature (London) **406**, 846 (2000); **399**, 354 (1999).
[4] B. L. Costelloa and A. Adamatzkyb, Chaos, Solitons Fractals **25**, 535 (2005); M. J. Meisner and G. N. Frantziskonis, *ibid.* **8**, 151 (1997).
[5] A. J. Lichtenberg and M. A. Lieberman, *Regular and Chaotic Dynamics* (Springer-Verlag, New York, 1992).
[6] J.-P. Eckmann, Rev. Mod. Phys. **53**, 643 (1981); J.-P. Eckmann and D. Ruelle, *ibid.* **57**, 617 (1985).
[7] S. NewHouse, D. Ruelle, and F. Takens, Commun. Math. Phys. **64**, 35 (1971).
[8] C. Grebogi, E. Ott, and J. A. Yorke, Phys. Rev. Lett. **51**, 339 (1983); Physica D **15**, 354 (1985).
[9] J. H. Curry and J. A. Yorke, Lect. Notes Math. **688**, 48 (1978).
[10] F. T. Arecchi, G. Giacomelli, A. Lapucci, and R. Meucci, Phys. Rev. A **43**, 4997 (1991).
[11] Z. Yu, J. Steinshnider, C. L. Littler, J. M. Perez, and J. M. Kowalski, Phys. Rev. E **49**, 220 (1994).
[12] J. J. Stagliano, Jr., J. M. Wersinger, and E. E. Slaminka, Physica D **92**, 164 (1996).
[13] A. Labate, M. Ciofini, and R. Meucci, Phys. Rev. E **57**, 5230 (1998).
[14] M. S. Baptista and I. L. Caldas, Phys. Rev. E **58**, 4413 (1998).
[15] M. S. Baptista and I. L. Caldas, Physica D **132**, 325 (1998).
[16] The saddle points herein and further in this paper represent an unstable periodic orbit visualized by maps of the flow.
[17] C. Letellier, A. Dinklage, H. El-Naggar, C. Wilke, and G. Bonhomme, Phys. Rev. E **63**, 042702 (2001).
[18] M. S. Baptista, T. P. Silva, J. C. Sartorelli, I. L. Caldas, and E. Rosa, Jr., Phys. Rev. E **67**, 056212 (2003).
[19] The perturbation is introduced in the oscillator set with a parameter far enough from the bifurcation point in the parameter space. In this region the phase space is robust under small perturbations.
[20] P. So, E. Ott, S. J. Schiff, D. T. Kaplan, T. Sauer, and C. Grebogi, Phys. Rev. Lett. **76**, 4705 (1996).
[21] M. Frank and M. Schmidt, Phys. Rev. E **56**, 2423 (1997).